Peierls to superfluid crossover in the one-dimensional, quarter-filled Holstein model

2013 J. Phys.: Condens. Matter 25 014005

(http://iopscience.iop.org/0953-8984/25/1/014005)

IOP PUBLISHING JOURNAL OF PHYSICS: CONDENSED MATTER
J. Phys.: Condens. Matter **25** (2013) 014005 (6pp) doi:10.1088/0953-8984/25/1/014005

Peierls to superfluid crossover in the one-dimensional, quarter-filled Holstein model

M Hohenadler and F F Assaad

Institut für Theoretische Physik und Astrophysik, Universität Würzburg, Am Hubland, D-97074 Würzburg, Germany

E-mail: martin.hohenadler@physik.uni-wuerzburg.de

Received 13 June 2012, in final form 19 July 2012
Published 5 December 2012
Online at stacks.iop.org/JPhysCM/25/014005

Abstract
We use continuous-time quantum Monte Carlo simulations to study retardation effects in the metallic, quarter-filled Holstein model in one dimension. Based on results which include the one- and two-particle spectral functions as well as the optical conductivity, we conclude that with increasing phonon frequency the ground state evolves from one with dominant diagonal order—$2k_F$ charge correlations—to one with dominant off-diagonal fluctuations, namely s-wave pairing correlations. In the parameter range of this crossover, our numerical results support the existence of a spin gap for all phonon frequencies. The crossover can hence be interpreted in terms of preformed pairs corresponding to bipolarons, which are essentially localized in the Peierls phase, and 'condense' with increasing phonon frequency to generate dominant pairing correlations.

(Some figures may appear in colour only in the online journal)

1. Introduction

The concept of preformed fermion pairs or bosonic degrees of freedom which condense to form a superfluid can be found in many domains of correlated quantum many-body systems. Examples include the resonating valence bond theory of high-temperature superconductivity [1], Mott metal–insulator transitions in cold atoms [2], or transitions between charge-density-wave and superconducting states in the family of dichalcogenides [3]. In this paper, we show in the framework of the Holstein model that these concepts can be carried over to one dimension, where, in the absence of continuous symmetry breaking, the phase transition is replaced by a crossover.

Quantum lattice fluctuations play a crucial role in one dimension. For classical phonons (i.e., in the adiabatic limit), the Peierls instability leads to a $2k_F$ periodic lattice deformation, resulting in corresponding charge ordering of electron pairs (bipolarons) and the opening of a gap at the Fermi level. In contrast, for the Holstein model, one can argue and give numerical evidence [4] that quantum phonons will close the charge gap but preserve the spin gap, thereby giving rise to a 'bad metal' state. In the latter, electrons bind into pairs and are mostly localized in the $2k_F$ charge order pattern. This results in a very high effective charge-carrier mass or, equivalently, in a very small Drude weight. We refer to this state as 'the Peierls state', which is to be distinguished from an insulating Peierls state with long-range charge order [5]. The latter has been studied intensely in Holstein-type models with and without spin, see discussion in section 2. The metallic Peierls state may be regarded as a more general concept for quasi-one-dimensional systems, applicable to noncommensurate fillings or the normal state ($T > T_c$) of a Peierls insulator [6]. On the level of bosonization, a metallic state with dominant $2k_F$ charge correlations requires a finite spin gap [6]. In the anti-adiabatic limit, the lattice adjusts instantaneously to the electronic motion, and the Holstein model maps onto the attractive Hubbard model with dominant pairing correlations.

The question addressed in this paper is the nature of the crossover from the adiabatic to the anti-adiabatic regime. The limiting cases of low (but finite) and high (or infinite) phonon frequency can be described as a Luther–Emery liquid [7, 8], corresponding to a Luttinger liquid with a gapless charge

mode and a gapped spin mode. A key result of the present work is that the crossover occurs without a closing of the spin gap, which suggests that the bipolarons existing in the Peierls state do not dissociate as a function of phonon frequency but instead constitute the preformed pairs of the superfluid phase.

The paper is organized as follows. In section 2 we introduce the model and explain the key ideas of the continuous-time quantum Monte Carlo method. Numerical results are presented in section 3, and we end with conclusions and a discussion of open issues and future research directions in section 4.

2. Model and method

The one-dimensional Holstein model is defined by the Hamiltonian [9]

$$\hat{H} = \sum_{k\sigma} \epsilon_k \hat{c}^\dagger_{k\sigma} \hat{c}_{k\sigma} + \sum_i \left(\frac{1}{2M} \hat{P}_i^2 + \frac{K}{2} \hat{Q}_i^2 \right) - g \sum_i \hat{Q}_i (\hat{n}_i - 1), \quad (1)$$

with the tight-binding dispersion relation $\epsilon_k = -2t\cos(ka) - \mu$ and the chemical potential μ. The operator $\hat{c}^\dagger_{i\sigma}$ creates an electron in the Wannier state centred on lattice site i with spin σ, $\hat{c}^\dagger_{k\sigma} = L^{-1/2} \sum_j \mathrm{e}^{ikj} \hat{c}^\dagger_{j\sigma}$ creates an electron in a Bloch state with wavevector k and spin σ, and $\hat{n}_i = \sum_\sigma \hat{c}^\dagger_{i\sigma} \hat{c}_{i\sigma}$ is the particle number operator; $\hat{Q}_i$ and $\hat{P}_i$ denote the displacement and momentum of the harmonic oscillator at site i.

To solve this model numerically without approximations (except for the finite system size), we integrate out the phonons at the expense of a retarded density–density interaction. The partition function of the resulting model is given by the path integral

$$Z = \int [\mathrm{d}c^\dagger \mathrm{d}c] \mathrm{e}^{-(S_0 + S_{\mathrm{ep}})} \quad (2)$$

with the following contributions to the action:

$$S_0 = \int_0^\beta \mathrm{d}\tau \sum_{i,j,\sigma} c^\dagger_{i\sigma}(\tau)(\delta_{ij}\partial_\tau - t_{ij}) c_{j\sigma}(\tau), \quad (3)$$

where $t_{ij} = 1$ for nearest neighbours and zero else, and

$$S_{\mathrm{ep}} = \int_0^\beta \mathrm{d}\tau \int_0^\beta \mathrm{d}\tau' \sum_{i,j} [n_i(\tau) - 1] D_0(i-j, \tau - \tau') \times [n_j(\tau') - 1]. \quad (4)$$

Here, $c^\dagger_{i\sigma}(\tau)$ is a Grassmann variable, β denotes the inverse temperature, and $D_0(i-j, \tau - \tau')$ is the phonon propagator. For dispersionless Einstein modes, D_0 is diagonal in space and takes the form

$$D_0(i-j, \tau - \tau') = \delta_{ij} \frac{g^2}{2k} P(\tau - \tau'), \qquad P(\tau) = \frac{\omega_0}{2} \frac{\mathrm{e}^{-|\tau|\omega_0} + \mathrm{e}^{-(\beta - |\tau|)\omega_0}}{1 - \mathrm{e}^{-\beta\omega_0}}. \quad (5)$$

The phonon frequency is given by $\omega_0 = \sqrt{K/M}$. In the following, we use t as the unit of energy, and set $\hbar$ and the lattice constant to unity.

In the fermionic form given by equations (3) and (4), the problem can be solved very efficiently by means of interaction expansion continuous-time quantum Monte Carlo methods [10–12]. The advantage of such a formulation is that we do not have to sample the lattice degrees of freedom directly, thereby eliminating the need for a Hilbert space cutoff. The details of the implementation of this algorithm can be found in [13]. The CTQMC method has previously been applied to the spinless [14] and the spinful Holstein model [15], as well as to a model with nonlocal electron–phonon interaction [16]. Simulations are carried out on one-dimensional lattices of length L using periodic boundary conditions.

The one-dimensional, half-filled Holstein model—with or without an additional Hubbard term to describe electron–electron repulsion—has been studied for many years. The existence of a metal–insulator transition at zero temperature has been established with the help of exact numerical methods, including quantum Monte Carlo [17–20, 16] the density-matrix renormalization group [4, 21–25] and exact diagonalization [26]. An overview of analytical work on the Peierls transition can be found in [27]. Many aspects of the relevant physics can also be captured by a spinless model with filling $n = 0.5$, including an extended metallic region in the phase diagram [28–31], the renormalization of the phonon mode [30, 32–34], and soliton excitations [14]. Retardation effects in the half-filled Holstein model were discussed, for example, in [35, 36], and for the spin-Peierls transition in [37].

Here we study the effect of phonon frequency in the quarter-filled Holstein model at a fixed electron–phonon coupling strength. For quarter filling and low phonon frequencies, the absence of first-order umklapp scattering—dominant at half filling—suppresses the Peierls instability, and stabilizes a state with gapless charge but gapped spin degrees of freedom, as well as a nonzero single-particle excitation gap, and dominant but critical $2k_{\mathrm{F}}$ charge correlations (a Luther–Emery liquid with interaction parameter $K_\rho < 1$). The spin gap is a result of backscattering. Signatures of this Luther–Emery phase have also been observed in the Holstein–Hubbard model with comparable electron–phonon and electron–electron interactions [38, 18, 19, 22, 23]. Our results presented below suggest that in contrast to half filling, we can observe dominant pairing correlations for high phonon frequencies at a commensurate density; dominant pairing for incommensurate filling has been reported before [39]. Recently, the existence of a correlated singlet state in the Holstein–Hubbard model away from half filling has been suggested [40, 41]. Compared to half filling, the critical value for the transition to a Peierls insulator is significantly larger at quarter filling [19]. This increase may be understood in terms of a devil's staircase, similar to charge-density-wave transitions in extended Hubbard models away from half filling [8]. As for half filling, the critical value of the electron–phonon coupling strength for the

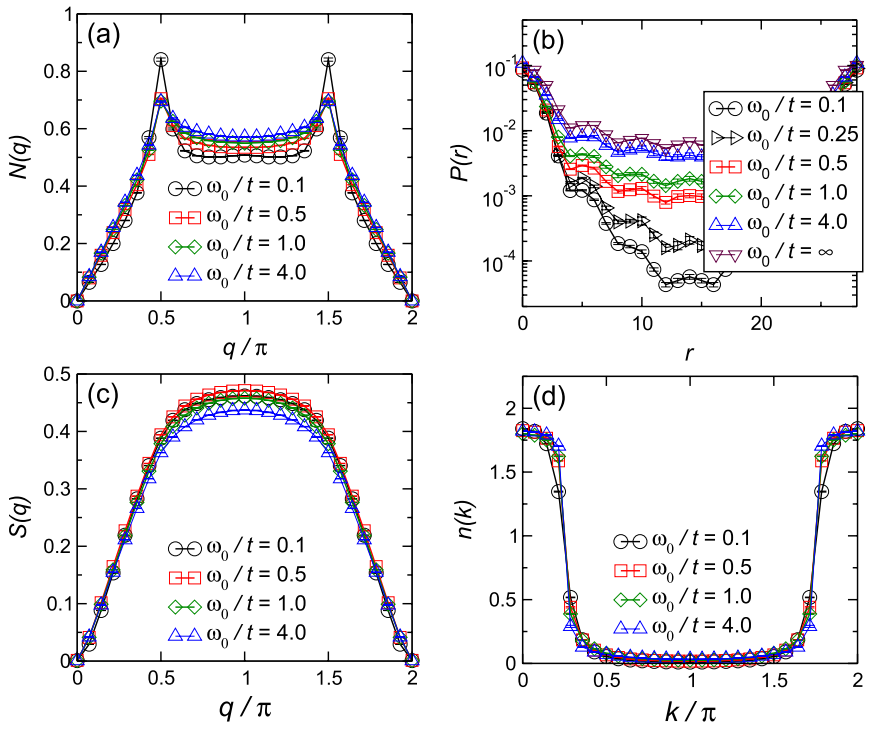

Figure 1. Static correlation functions for different values of the phonon frequency ω_0/t at $\lambda = 0.35$, and for a quarter-filled band ($n = 0.5$). The panels show (a) the charge structure factor, (b) the pairing correlator, (c) the spin structure factor, and (d) the momentum distribution function. Here $L = 28$ and $\beta t = 40$.

metal–insulator transition increases with increasing phonon frequency as a result of enhanced lattice fluctuations [39].

3. Results

In the anti-adiabatic limit $\omega_0 \to \infty$, $P(\tau)$ in equation (5) reduces to a Dirac δ-function, facilitating the above-mentioned mapping of the Holstein model onto the attractive Hubbard model, with $U = g^2/k$. The ratio of this binding energy and the bandwidth $W = 4t$ gives the dimensionless electron–phonon coupling

$$\lambda = \frac{g^2}{kW}. \tag{6}$$

Throughout this paper, we set $\lambda = 0.35$ and concentrate on the quarter-filled band with $k_F = \pi/4$. In the following, we first establish a picture of the physics on the basis of equal-time correlation functions, and then turn to dynamical correlations.

3.1. Static correlation functions

Figure 1 shows equal-time correlation functions for charge, spin, and pairing, as well as the momentum distribution function, at various phonon frequencies. In the adiabatic limit $\omega_0/t = 0$, any $\lambda > 0$ leads to an insulating state. As discussed in section 2, we choose the coupling strength $\lambda = 0.35$ such that we have a metallic Luther–Emery liquid with dominant $2k_F$ charge correlations for low phonon frequencies, and then study the evolution as a function of increasing ω_0/t. In particular, we have verified that for $\omega_0/t = 0.1$, the lowest nonzero frequency considered in the following, there is no long-range order; this can be seen from the finite-size dependence of the charge susceptibility [19].

The density (or charge) structure factor, defined as

$$N(q) = \sum_r e^{iqr}(\langle \hat{n}_r \hat{n}_0 \rangle - \langle \hat{n}_r \rangle \langle \hat{n}_0 \rangle), \tag{7}$$

is plotted in figure 1(a). For classical phonons, $\omega_0 = 0$, the Peierls instability leads to long-range $2k_F$ charge order at zero temperature. As discussed above, quantum lattice fluctuations (occurring for $\omega_0 > 0$) can melt this order, and lead to a state with dominant but power-law $2k_F$ charge correlations [15], as confirmed by the cusp at $2k_F = \pi/2$ in figure 1(a). The magnitude of the peak at $q = 2k_F$ initially decreases and then saturates upon increasing the phonon frequency, signalling competing ordering mechanisms as well as enhanced lattice fluctuations. The linear form of the charge structure factor at long wavelengths (see figure 1(a)) indicates a $1/r^2$ power-law decay of the real-space charge correlations and hence a metallic state.

In figure 1(b), we present the pair correlation function in the onsite s-wave channel,

$$P(r) = \langle \hat{\Delta}_r^\dagger \hat{\Delta}_0 \rangle, \qquad \hat{\Delta}_r^\dagger = \hat{c}_{r\uparrow}^\dagger \hat{c}_{r\downarrow}^\dagger. \tag{8}$$

In contrast to the density correlator which picks up diagonal order, $P(r)$ detects off-diagonal order characteristic of a superconducting state. In the Peierls state obtained for classical phonons, diagonal long-range charge order leads to an exponential decay of pairing correlations at long distances. The fluctuations resulting from a finite phonon frequency

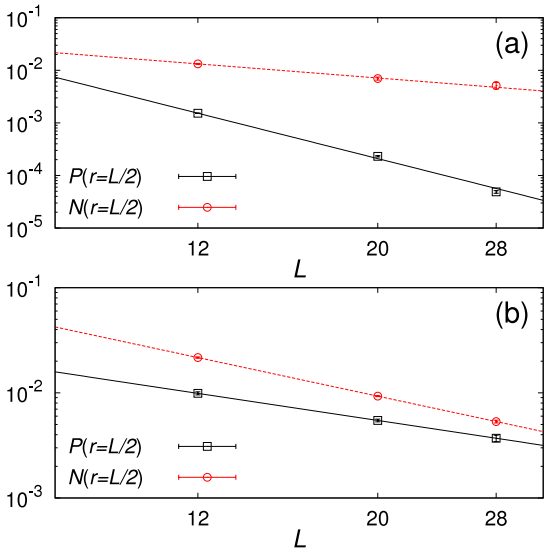

Figure 2. Pairing (□) and charge-density-wave (◯) correlations at the largest distance $r = L/2$ for different system sizes L. Here $\lambda = 0.35$, $\beta t = L$ and (a) $\omega_0/t = 0.1$, (b) $\omega_0/t = 4$. Lines are fits to the form $f(r) = A/r^{\eta}$.

close the charge gap, and render the pairing correlations critical. Comparing figures 1(a) and (b), we see that the suppression of the $2k_F$ charge correlations is accompanied by an increase of the pairing correlations, especially at large distances. A possible interpretation is that with increasing phonon frequency, the trapping of bipolarons in the $2k_F$ lattice modulation gives way to a 'condensation' (in the usual sense of superfluidity in one dimension) of those preformed pairs.

The above interpretation relies on the electron pairs remaining bound upon increasing the phonon frequency. Evidence for the existence of bound pairs is provided by the equal-time spin–spin correlation function

$$S(q) = \sum_r e^{iqr} \langle \hat{S}^z_r \hat{S}^z_0 \rangle, \tag{9}$$

which we show in figure 1(c). For all values of the phonon frequency, the cusps at $q = 0$ and $q = 2k_F$ are smeared out, thus lending support to an exponential decay of the spin correlations. The presence of a spin gap will be explicitly confirmed by results for the dynamical spin structure factor below.

Finally, we plot in figure 1(d) the momentum distribution function

$$n(k) = \sum_\sigma \langle \hat{c}^\dagger_{k\sigma} \hat{c}_{k\sigma} \rangle. \tag{10}$$

Following the above interpretation, we expect a smooth variation of this quantity as a function of wavevector k. In particular we do not expect any nonanalytical behaviour at $k = k_F$ or $k = 3k_F$. For classical phonons, the smooth variation of $n(k)$ stems from the nonzero single-particle gap of the Peierls state. In the anti-adiabatic limit, where the model maps onto the attractive Hubbard model, this behaviour is equally expected since it is known that the ground state is a Luther–Emery liquid with gapped single-particle

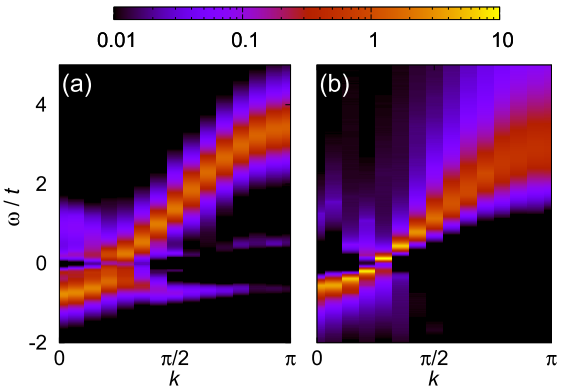

Figure 3. Single-particle spectral function $A(k, \omega)$ for (a) $\omega_0/t = 0.1$ and (b) $\omega_0/t = 4$. Here $\lambda = 0.35$, $n = 0.5$, $L = 28$, and $\beta t = 28$.

excitations [8]. Since we observe a continuous crossover from low to high frequencies in figure 1(d), we argue that our data supports the existence of a single-particle gap for all considered values of ω_0; this is confirmed in figure 3 and discussed in the following subsection.

Our analysis of the equal-time correlation functions in this section suggests the existence of a crossover from dominant diagonal (charge-density-wave) to dominant off-diagonal (pairing) fluctuations as a function of the phonon frequency. This evolution is confirmed by the results for $P(r)$ and $N(r) = \langle \hat{n}_r \hat{n}_0 \rangle - \langle \hat{n}_r \rangle \langle \hat{n}_0 \rangle$ shown in figure 2, where we plot these two correlators at the largest distance $r = L/2$ for different L. Whereas for $\omega_0/t = 0.1$ the charge correlations decay significantly slower than the pairing correlations, see figure 2(a), dominant pairing correlations can be seen for $\omega_0/t = 4$ in figure 2(b). The ratio of the exponents obtained from least-square fits is $\eta_{CDW}/\eta_{SS} \approx 0.3$ for $\omega_0/t = 0.1$, and $\eta_{CDW}/\eta_{SS} \approx 1.4$ for $\omega_0/t = 4$.

3.2. Dynamical correlation functions

With the help of a stochastic analytical continuation scheme [42], we can extract momentum and frequency dependent spectral functions from the imaginary time Green's functions accessible in the quantum Monte Carlo simulations. Here we consider the single-particle spectral function

$$A(k, \omega) = \frac{1}{Z} \sum_{n,m} (e^{-\beta E_n} + e^{-\beta E_m}) \times |\langle n|\hat{c}_{k\sigma}|m\rangle|^2 \delta(E_n - E_m - \omega), \tag{11}$$

the dynamical charge structure factor

$$N(q, \omega) = \frac{\pi}{Z} \sum_{n,m} e^{-\beta E_m} |\langle n|\hat{n}_q|m\rangle|^2 \delta(E_n - E_m - \omega), \tag{12}$$

where $\hat{n}_q = L^{-1/2} \sum_j e^{iqj} \hat{n}_j$ and with the sum rule $N(q) = \pi^{-1} \int d\omega\, N(q, \omega)$, and the dynamical spin structure factor $S(q, \omega)$ defined as in equation (12) but with $\hat{n}_q$ replaced by $\hat{S}^z_q$.

The results for $A(k, \omega)$ shown in figure 3 reveal the existence of a spin gap both at low ((a), $\omega_0/t = 0.1$) and high

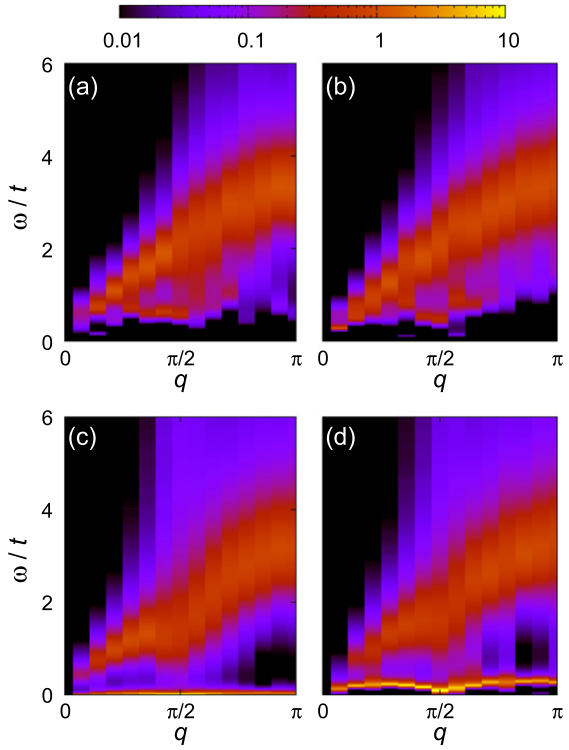

Figure 4. Dynamical spin (a), (b) and charge (c), (d) structure factors for (a), (c) $\omega_0/t = 0.1$ and (b), (d) $\omega_0/t = 0.5$. Here $\lambda = 0.35$, $n = 0.5$, $L = 28$, and $\beta t = 40$.

((b), $\omega_0/t = 4$) phonon frequencies, although the size of the gap is smaller in figure 3(b) than in figure 3(a). Very similar results have previously been obtained for $\omega_0/t = 0.1$ [15].

The nonzero spin gap is confirmed by our results for the dynamical spin structure factor $S(q, \omega)$ in figure 4(a) (for $\omega_0/t = 0.1$) and figure 4(b) (for $\omega_0/t = 0.5$), which reveal the absence of low-lying spectral weight near $q = 0$.

The suggested crossover from a Peierls to a superconducting state is expected to be reflected in an enhancement of the mobility of the preformed pairs. For the two values of the phonon frequency considered here ($\omega_0/t = 0.1, 0.5$), the dynamical charge structure factor in figures 4(c) and (d) shows two features: a high-energy particle–hole continuum reminiscent of the noninteracting problem, and a low-lying excitation band. At $\omega_0/t = 0.1$, figure 4(c), the dispersion of the latter is extremely flat and within our resolution we cannot distinguish the associated charge velocity from zero. This narrow mode reflects the very slow dynamics of bipolarons which are predominantly localized to form the $2k_F$ charge-density-wave order. At a higher phonon frequency, $\omega_0/t = 0.5$, see figure 4(d), a clear dispersion relation with a minimum at $q = 2k_F$ emerges.

The enhancement of the velocity of the bipolarons as a function of phonon frequency is also apparent in the optical conductivity, defined as

$$\sigma'(\omega) = \frac{\pi}{Z\omega} \sum_{n,m} \mathrm{e}^{-\beta E_m}(1 - \mathrm{e}^{-\beta\omega}) \times |\langle n|\hat{j}|m\rangle|^2 \delta(E_n - E_m - \omega), \qquad (13)$$

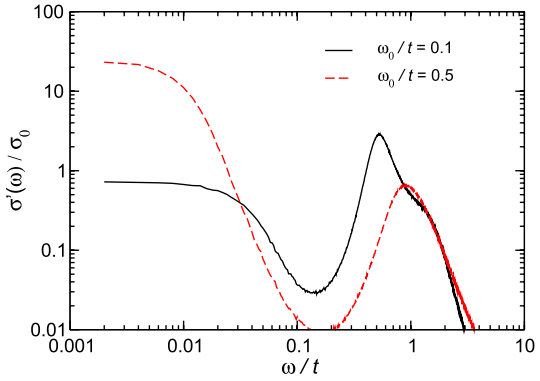

Figure 5. Optical conductivity for $\omega_0/t = 0.1$ (—) and $\omega_0/t = 0.5$ (– – – –). Here $\lambda = 0.35$, $n = 0.5$, $L = 28$, $\beta t = 40$, and $\sigma_0 = e^2/2\pi$.

with the paramagnetic current operator $\hat{j} = it\sum_{i\sigma}(\hat{c}^\dagger_{i\sigma}\hat{c}_{i+1\sigma} - \text{H.c.})$. Results for $\sigma'(\omega)$ are plotted in figure 5, and reveal that the Drude weight is enhanced by an order of magnitude upon increasing the phonon frequency from $\omega_0/t = 0.1$ to $\omega_0/t = 0.5$.

The enhancement of the Drude peak follows directly from the dynamical charge structure factor. Using the continuity equation, the optical conductivity and the dynamical charge structure factor are related via [15]

$$\sigma'(q, \omega) = \frac{\omega}{q^2}(1 - \mathrm{e}^{-\beta\omega})N(q, \omega). \qquad (14)$$

In the long-wavelength limit, we can make the approximation $N(q, \omega) \propto q\delta(\omega - v_c q)$. Here, v_c is the charge velocity and the prefactor q stems from phase space available for long-wavelength charge fluctuations[1]. This ansatz leads to $\sigma'(q = 0, \omega) \propto v_c\delta(\omega)$, so that the enhancement of the velocity v_c is reflected in the conductivity.

4. Discussion and conclusions

We have presented results for static and dynamical correlation functions of the quarter-filled Holstein model at $\lambda = 0.35$, and concentrated on the evolution of the metallic state from the adiabatic to the anti-adiabatic limit. For all considered values of the phonon frequency, our data support the presence of a spin gap as a consequence of backward scattering. Such a system with a gapless charge mode and a gapped spin mode is described by the Luther–Emery fixed point. At the latter, the density and pairing correlators have the form [8]

$$\langle n(r)n(0)\rangle = \frac{A_0}{r^2} + \frac{A_1}{r^{K_\rho}}\cos(2k_F r) + \frac{A_2}{r^{4K_\rho}}\cos(4k_F r) + \cdots, \qquad (15)$$

$$\langle \Delta^\dagger(r)\Delta(0)\rangle = \frac{C}{r^{1/K_\rho}} + \cdots, \qquad (16)$$

in addition to an exponential decay of the spin–spin correlations. The dominant correlations are $2k_F$ density

[1] The factor q equally follows from the sum rule $\int \mathrm{d}\omega\, N(q, \omega) = N(q) \propto q$.

correlations for $K_\rho < 1$, and pairing correlations for $K_\rho > 1$. Our numerical results, in particular those shown in figure 2, are hence best understood in terms of an enhancement of K_ρ from values smaller than one at small ω_0/t (leading to dominant charge-density-wave correlations) to values larger than 1 in the nonadiabatic regime where we observe significantly larger pairing correlations. A quantitative finite-size scaling of K_ρ is difficult for several reasons, including the necessity to increase L in steps of eight, and the possible importance of logarithmic corrections as a result of retardation effects [20]. Nevertheless, a cubic extrapolation based on $L = 12, 20, 28$ gives $K_\rho \approx 0.8$ for $\omega_0/t = 0.1$ and $K_\rho \approx 1.1$ for $\omega_0/t = 4$.

Since the spin degrees of freedom always remain gapped, we have interpreted our results in terms of preformed pairs which are essentially localized in the $2k_F$ charge-density-wave state realized in the adiabatic limit. This localization leads to a metallic state with a small Drude weight. Upon increasing the phonon frequency, enhanced lattice fluctuations permit bipolaron motion, thereby providing a kinetic energy gain. The resulting state is characterized by a significantly larger Drude response or, equivalently, an enhanced bipolaron velocity.

A fruitful direction for future research concerning the evolution of the Peierls state is the effect of higher dimensions. By studying, for example, weakly coupled Holstein chains, the crossover from a charge-density-wave state to a superfluid discussed here may evolve into a phase transition expected to be in the *XY* universality class.

Acknowledgments

We acknowledge support from the DFG Grants No. Ho 4489/2-1 and FOR 1162, and generous computer time at the LRZ Munich and the Jülich Supercomputing Centre.

References

[1] Anderson P W, Lee P A, Randeria M, Rice T M, Trivedi N and Zhang F C 2004 *J. Phys.: Condens. Matter* **16** R755
[2] Greiner M, Mandel O, Esslinger T, Hänsch T W and Bloch I 2002 *Nature* **415** 39
[3] Sipos B, Kusmartseva A F, Akrap A, Berger H, Forro L and Tutis E 2008 *Nature Mater.* **7** 960
[4] Jeckelmann E, Zhang C and White S R 1999 *Phys. Rev.* B **60** 7950
[5] Peierls R 1979 *Surprises in Theoretical Physics* (Princeton, NJ: Princeton University Press)
[6] Voit J 1998 *Eur. Phys. J.* B **5** 505
[7] Emery V J 1979 Theory of the one-dimensional electron gas *Highly Conducting One-Dimensional Solids* ed J T Devreese (New York: Plenum) p 247
[8] Giamarchi T 2004 *Quantum Physics in One Dimension* (Oxford: Clarendon)
[9] Holstein T 1959 *Ann. Phys.* **8** 325
Holstein T 1959 *Ann. Phys.* **8** 343
[10] Rombouts S M A, Heyde K and Jachowicz N 1999 *Phys. Rev. Lett.* **82** 4155
[11] Rubtsov A N, Savkin V V and Lichtenstein A I 2005 *Phys. Rev.* B **72** 035122
[12] Gull E, Millis A J, Lichtenstein A I, Rubtsov A N, Troyer M and Werner P 2011 *Rev. Mod. Phys.* **83** 349
[13] Assaad F F and Lang T C 2007 *Phys. Rev.* B **76** 035116
[14] Hohenadler M, Fehske H and Assaad F F 2011 *Phys. Rev.* B **83** 115105
[15] Assaad F F 2008 *Phys. Rev.* B **78** 155124
[16] Hohenadler M, Assaad F F and Fehske H 2012 *Phys. Rev. Lett.* at press (arXiv:1205.0612)
[17] Hirsch J E and Fradkin E 1983 *Phys. Rev.* B **27** 4302
[18] Clay R T and Hardikar R P 2005 *Phys. Rev. Lett.* **95** 096401
[19] Hardikar R P and Clay R T 2007 *Phys. Rev.* B **75** 245103
[20] Tam K-M, Tsai S-W and Campbell D K 2011 *Phys. Rev.* B **84** 165123
[21] Zhang C, Jeckelmann E and White S R 1999 *Phys. Rev.* B **60** 14092
[22] Fehske H, Hager G and Jeckelmann E 2008 *Europhys. Lett.* **84** 57001
[23] Ejima S and Fehske H 2010 *J. Phys.: Conf. Ser.* **200** 012031
[24] Tezuka M, Arita R and Aoki H 2005 *Phys. Rev. Lett.* **95** 226401
[25] Matsueda H, Tohyama T and Maekawa S 2006 *Phys. Rev.* B **74** 241103
[26] Fehske H, Wellein G, Hager G, Weiße A and Bishop A R 2004 *Phys. Rev.* B **69** 165115
[27] Bakrim H and Bourbonnais C 2007 *Phys. Rev.* B **76** 195115
[28] Bursill R J, McKenzie R H and Hamer C J 1998 *Phys. Rev. Lett.* **80** 5607
[29] Weiße A and Fehske H 1998 *Phys. Rev.* B **58** 13526
[30] Hohenadler M, Wellein G, Bishop A R, Alvermann A and Fehske H 2006 *Phys. Rev.* B **73** 245120
[31] Ejima S and Fehske H 2009 *Europhys. Lett.* **87** 27001
[32] Creffield C E, Sangiovanni G and Capone M 2005 *Eur. Phys. J.* B **44** 175
[33] Sykora S, Hübsch A, Becker K W, Wellein G and Fehske H 2005 *Phys. Rev.* B **71** 045112
[34] Sykora S, Hübsch A and Becker K W 2006 *Europhys. Lett.* **76** 644
[35] Tam K-M, Tsai S-W, Campbell D K and Castro Neto A H 2007 *Phys. Rev.* B **75** 161103
[36] Fehske H, Holicki M and Weisse A 2000 Lattice dynamical effects on the peierls tansition in one-dimensional metals and spin chains *Advances in Solid State Physics* vol 40 (Berlin: Springer) pp 235–50
[37] Citro R, Orignac E and Giamarchi T 2005 *Phys. Rev.* B **72** 024434
[38] Takada Y and Chatterjee A 2003 *Phys. Rev.* B **67** 081102
[39] Tezuka M, Arita R and Aoki H 2007 *Phys. Rev.* B **76** 155114
[40] Reja S, Yarlagadda S and Littlewood P B 2011 *Phys. Rev.* B **84** 085127
[41] Reja S, Yarlagadda S and Littlewood P B 2011 arXiv:1111.6148
[42] Beach K S D 2004 arXiv:0403055